Journal of Solid State Chemistry 182 (2009) 3399–3405

Contents lists available at ScienceDirect

Journal of Solid State Chemistry

journal homepage: www.elsevier.com/locate/jssc

A twofold interpenetrating framework based on the α-metatungstates

Pengpeng Zhang [a], Jun Peng [a,*], Xiaoqing Shen [b], Zhangang Han [c], Aixiang Tian [a], Haijun Pang [a], Jingquan Sha [a], Yuan Chen [a], Min Zhu [a]

[a] Key Laboratory of Polyoxometalate Science of Ministry of Education, Faculty of Chemistry, Northeast Normal University, Changchun, Jilin, 130024, PR China
[b] Department of Chemistry, Zhengzhou University, Zhengzhou, Henan 450052, PR China
[c] Shijiazhuang, Hebei, Hebei Normal University, College of Chemistry & Material Science, PR China

ARTICLE INFO

Article history:
Received 16 April 2009
Received in revised form
20 September 2009
Accepted 28 September 2009
Available online 13 October 2009

Keywords:
α-metatungstate
Electrocatalytic activity
Interpenetrating framework
Thermal decomposition

ABSTRACT

A new compound based on polyoxometalates, $[Cu(bbi)]_5H[H_2W_{12}O_{40}]$ (**1**) (bbi=1,1′-(1,4-butanediyl)bis(imidazole)), has been hydrothermally synthesized and characterized by elemental analyses, IR spectroscopy, thermogravimetric analyses, and single X-ray diffraction. Compound **1** shows a twofold 3D+3D topology, and it represents the first interpenetrating network based on the isopolytungstate. The electrochemical property of compound **1** modified carbon paste electrode (**1**−CPE) was investigated in 1 M H_2SO_4 solution, and the results indicate that **1**−CPE exhibits the electrocatalytic activity toward the reduction of bromate and nitrite. Further, the non-isothermal kinetics of the thermal decomposition of compound **1** provides the dynamic parameters *E* (activation energy) and *A* (pre-exponential factor) for the pyrolytic reaction of the organic ligands.

1. Introduction

Entangled systems have captured chemists' interest owing to not only their intrinsic aesthetic characters but also their promising potential applications as functional solid state materials [1–11]. Among the various types of the entangled systems, interpenetrating networks are the most studied [12–20]. Systematical reviews of the appealing interpenetration have been made by Ciani, Robson and Batten [21–23], in which interpenetrating network structures were defined as infinite, ordered polycatenanes or polyrotaxanes. In addition, the interpenetrating individual motifs could not be separated except for breaking one of them. Recently, the interpenetrating networks of the metal organic coordination polymers have been reported in an increasing frequency, which greatly enrich the entangled system [24–33].

Polyoxometalates (POMs), as a unique class of inorganic metal-oxide clusters, possess intriguing structures, unexpected reactivity, and abundant potential applications [34–42]. Due to these special abilities, especially their potential multiple coordination sites, POMs are usually employed as inorganic building blocks connecting metal-organic frameworks (MOFs) to construct various frameworks with attractive topologies and high dimensionality [43–47]. However, compared with the successful synthesis of other MOF-modified POMs, such as Keggin, Wells–Dawson, Anderson and isopolymolybdates [48–51], those based on the isopolytungstates are rarely explored, especially for the 3D frameworks [52,53]. So plenty room is remained to design and synthesize high-dimensional MOF-modified isopolytungstates with novel architectures and characteristics such as fluorescence, magnetism and sorption [52–54]. Further, along with the evolution of metal organic coordination polymers with entangled networks, such structures based on POMs and appropriate MOFs are in progress [55–60].

Our previous work has verified that the synergetic interactions of the POM coordination sites, the flexibility of the ligand and the coordination characteristics of the metal cations can give rise to complex networks with big voids [43,50]. The interpenetrating frameworks are often formed by the occupancy of the large voids of one framework by one or more other networks. Due to the large volume of POMs, the choice of longer organic ligands seems to be essential for the synthesis of frameworks with large voids. The bbi ligand (1,1′-(1,4-butanediyl)bis(imidazole)) attracts our attention, in which the flexible segment $-(CH_2)_4-$ can bend or rotate to accommodate the coordination environments of POMs and the metal cations [43,57,58]. So, the bbi is an excellent synthon for the construction of interpenetrating networks. Cu(I) cation also is a good candidate with variable coordination numbers and tunable coordination spheres.

Based on the above mentioned consideration, we chose $Na_2WO_4\cdot 2H_2O$, $Cu(OAc)_2\cdot H_2O$, and bbi as starting materials, tried to obtain interpenetrating structures based on isopolytungstate under hydrothermal condition. As expected, α-metatungstate was generated and a new compound with a twofold

* Corresponding author. Fax: +86 431 85099667.
E-mail addresses: jpeng@nenu.edu.cn, pjun56@yahoo.com (J. Peng), tianax717@nenu.edu.cn (A. Tian).

0022-4596/$ - see front matter © 2009 Elsevier Inc. All rights reserved.
doi:10.1016/j.jssc.2009.09.032

interpenetrated 3D+3D topology, $[Cu(bbi)]_5H[H_2W_{12}O_{40}]$, was obtained. To the best of our knowledge, it represents the first example of interpenetrating network based on the isopolytungstates.

2. Experimental section

2.1. General procedures

All reagents were purchased commercially and used without further purification. The ligand bbi was prepared according to the reported procedure [61]. Elemental analyses (C, H, N) were performed on a Perkin-Elmer 2400 CHN Elemental Analyzer, Cu and W were analyzed on a PLASMA-SPEC(I) ICP atomic emission spectrometer. The IR spectra were obtained on an Alpha Centaurt FT/IR spectrometer with KBr pellets in the $400-4000\,cm^{-1}$ region. The thermal gravimetric analyses (TGA) were carried out on the NETZCH TG209 instrument in flowing N_2. Cyclic voltammograms were obtained with a CHI 660 electrochemical workstation at room temperature. Platinum gauze was used as a counter electrode and Ag/AgCl electrode was referenced. Chemically bulk-modified carbon paste electrode (CPE) was used as working electrode.

2.2. Synthesis of the compound

A mixture of $Na_2WO_4\cdot 2H_2O$ (5 mmol), $Cu(OAc)_2\cdot H_2O$ (2 mmol), bbi (2 mmol), triethylamine (trea) (0.2 mmol) and H_2O 10 mL was stirred for 1 h at room temperature. The pH was adjusted to about 4.5 with 1 M NaOH and 1 M HCl, and then the mixture was transferred to an 18 mL Teflon-lined reactor and kept under autogenous pressure at 170 °C for 5 days. The reactor was slowly cooled to room temperature over a period of 10 °C/h. Brown block crystals of **1** were filtered, washed with water, and dried at room temperature. Yield: 60% based on Cu. $C_{50}H_{73}Cu_5N_{20}O_{40}W_{12}$ (4118.04): Calcd: C, 14.58; H, 1.79; N, 6.80; Cu, 7.72; W, 53.57%; Found: C, 14.61; H, 1.68; N, 6.74; Cu, 7.79; W, 53.51%; IR (solid KBr pellet, cm^{-1}): 3735 (w), 3425 (s), 3114 (m), 2939 (w), 1633 (m), 1515 (s), 1441 (m), 1277 (m), 1232 (m), 1108 (s), 949 (s), 876 (s), 774 (s), 656 (w), 509 (w).

2.3. Preparation of 1 – CPE

Compound **1** modified carbon paste electrode **1** – CPE was prepared as follows: 90 mg of graphite powder and 8 mg of compound **1** were mixed and ground together by agate mortar and pestle to achieve a uniform mixture, and then 0.1 mL nujol was added with stirring. The homogenized mixture was packed into a glass tube with 1.5 mm inner diameter, and the tube surface was wiped with paper. Electrical contact was established with copper rod through the back of the electrode. Ag/AgCl (3 M KCl) electrode was used as a reference electrode, and a Pt wire as a counter electrode.

2.4. X-ray crystallography

Crystal data for compound **1** were collected on a Bruker SMART-CCD diffractometer, with Mo$K\alpha$ monochromatic radiation (λ=0.71073 Å) at 293 K, respectively. The structure was solved by the direct methods and refined by full matrix least-squares on F^2 using the SHELXTL crystallographic software package [62,63]. The positions of hydrogen atoms on carbon atoms were calculated theoretically. Crystallographic data are given in Table 1. Crystallographic data for the structure reported in this paper have been deposited in the Cambridge Crystallographic Data Center with CCDC number 710054 for **1**.

Table 1
Crystal data and structure refinements for compound **1**.

Compounds	**1**
Empirical formula	$C_{50}H_{73}Cu_5N_{20}O_{40}W_{12}$
Mr	4118.04
Temp (K)	296(2)
Wavelength (Å)	0.71073
Crystal system	monoclinic
Space group	$P2(1)/n$
a (Å)	14.276(6)
b (Å)	14.235(6)
c (Å)	20.828(8)
β (°)	91.258(5)
V (Å^3)	4232(3)
Z	2
Dc (mg cm^{-3})	3.229
μ(Mo$K\alpha$) (mm^{-1})	17.552
Final R_1[a],	0.0522
wR_2[b] [$I>2\sigma(I)$]	0.1134
Goodness of fit	1.058

[a] $R_1=\sum||F_o|-|F_c||/|F_o|$.
[b] $wR_2=\{\sum w(F_o^2-F_c^2)^2]/\sum[w(F_o^2)^2]\}^{1/2}$.

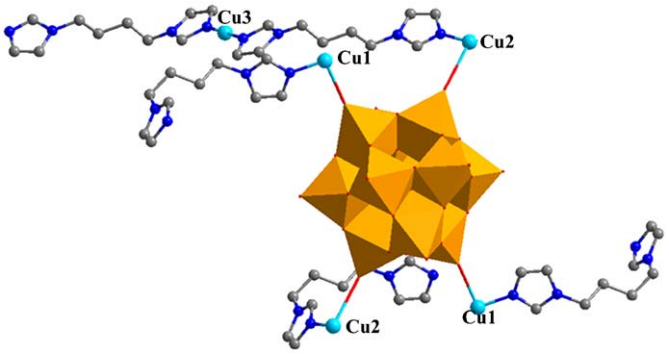

Fig. 1. Stick/polyhedral view of the fundamental building block of compound **1**. The hydrogen atoms are omitted for clarity.

3. Result and discussion

Compound **1** was hydrothermally synthesized from the reactant $Na_2WO_4\cdot 2H_2O$, $Cu(OAc)_2\cdot H_2O$, bbi and trea. The copper atoms in compound **1** are in the +I oxidation state, confirmed by charge balance, coordination environments, bond valence sum (BVS) calculations [64], and crystal color. All W atoms are in the +VI oxidation state. The change of $Cu^{II}\rightarrow Cu^{I}$ may be due to the addition of reductant trea, which is usual under hydrothermal conditions [65,66]. An additional proton was assigned as an external counteraction of α-metatungstate $[H_2W_{12}O_{40}]^{6-}$, so compound **1** was formulated as $[Cu(bbi)]_5H[H_2W_{12}O_{40}]$ [67].

3.1. Crystal structure of compound 1

Single crystal X-ray diffraction analysis reveals that the asymmetric unit of compound **1** contains one α-$H[H_2W_{12}O_{40}]^{5-}$ (abbreviated as W_{12}) cluster, five Cu^{I} cations and five bbi molecules (Fig. 1).

The W_{12} cluster is a protonated α-metatungstate $[H_2W_{12}O_{40}]^{6-}$, in which the twelve WO_6 octahedra are arranged

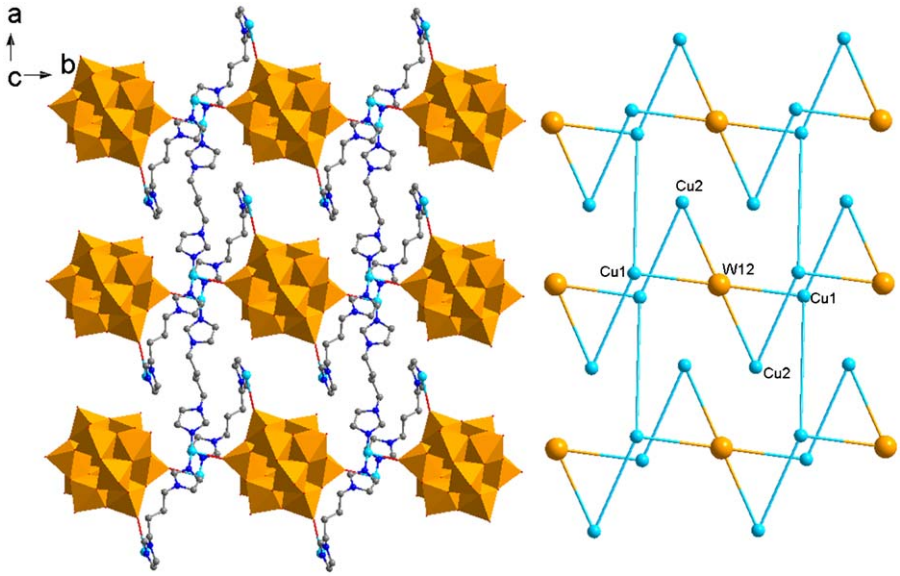

Fig. 2. Left: The 2D layer in the 3D framework of compound **1**. Right: The topological representation of the layer.

in four edge-shared $\{W_3O_{13}\}$ triplets, the four $\{W_3O_{13}\}$ triplets are connected with each other by vertices, just as in the Keggin type polyanions. Differently, two protons replace their central heteroatom taking up the central cavity. The third proton was assigned as an external counter cation. The oxygen atoms in the W_{12} cluster could be classified into four kinds: the central oxygen atoms which linked three WO_6 octahedra; the bridging oxygen atoms which are shared by two WO_6 octahedra; the terminal oxygen atoms belonged to one WO_6 octahedra; the terminal oxygen atoms further coordinated to Cu cations. (Selected bond lengths and angles are shown in the Supporting Information Table S1) The bond distances are in accord with those in the reported works [52,53].

There are three kinds of Cu^I cations in the asymmetric unit: Cu1, Cu2 and Cu3. Cu1 and Cu2 cations are coordinated with two N atoms from two bbi molecules and one terminal oxygen atom of the W_{12} cluster to form the "T-type" geometry. The Cu3 cation coordinates to two N atoms from two bbi molecules and exhibits the linear geometry. Cu2 and Cu3 cations are disordered over two adjacent positions with occupancies of 0.5, respectively [68,69]. All the bbi molecules in compound **1** adopt the bidentate bridging coordination mode to link two Cu^I cations through the imidazole nitrogen atoms. Firstly, each W_{12} cluster acts as quadridentate inorganic ligand coordinating to two Cu1 and two Cu2 cations via four terminal oxygen atoms. The bbi ligands link Cu1 and Cu2 cations, forming a Cu–bbi–Cu bridge which fuses the adjacent W_{12} clusters and leads to the formation of a 1D infinite chain (Fig. S1). These chains are further linked by bbi ligands into an infinite 2D layer through coordinating to the Cu1 cations in the neighboring lines (Fig. 2). The 2D layers stack parallel along the *c* axis, then the Cu3 cations and the bbi ligands covalently connect the adjacent layers into a 3D framework. Here the bbi ligand offers one nitrogen atom to coordinate to a Cu3 cation and the other nitrogen atom to link a Cu2 cation in the 2D layer (Fig. 2 left).

From the topological view, the W_{12} cluster is considered as a four connected node, both the Cu1 and Cu2 atoms are considered as three connected nodes, Cu3 atom is the two connected bridging node, and the bbi molecules act as linkages. As a result, the structure shows a 3D (3,3,4)−connected framework with the $(6^18^2)_2(6^28^210^2)$ topology (Fig. 3 right).

Seen from Fig. 3, there are big voids in the 3D framework. As is known, large structural voids are often occupied by solvent molecules or guest molecules to achieve the structural stabilization. Otherwise, the interpenetration phenomena may occur, that is, the voids associated with one framework are occupied by one or more independent frameworks to fill the spaces. Interestingly, in the structure of compound **1**, the voids in the 3D framework are occupied by a second framework. Notably, the second framework is identical to the first one, giving a twofold 3D+3D interpenetrating structure (Fig. 4). In the interpenetrating structure, each 3D framework is self-closed, that means, two 3D networks coexist, which are not bonded chemically but cannot be separated except for breaking one of them (Fig. S2). To the best of our knowledge, seldom examples of such interpenetrating structure based on POMs have been reported [70–72], and compound **1** represents the first example of interpenetrating structure based on the isopolytungstate.

3.2. FTIR and XPRD spectroscopy

The IR spectrum of compound **1** is shown in Fig. S3. Characteristic bands at 949, 876, 774, 656, 509 cm^{-1} for **1** are attributed to $\nu(W{=}O)$ and $\nu(W{-}O{-}W)$, respectively. Bands in the region of 1100–1700 cm^{-1} are attributed to the bbi ligand. There are some slight changes in peak position, perhaps due to coordination [73].

The XRPD pattern for compound **1** is presented in Fig. S4. The diffraction peaks of the simulated and experimental pattern match well, indicating the phase purity of the compound **1**.

3.3. Thermogravimetric analysis

The thermogravimetric analysis of compound **1** was determined under the nitrogen atmosphere. Meanwhile the TG experiment for organic compound bbi was carried out for comparison. In the TG curve of bbi, neglecting the mass loss below 100 °C, a huge mass loss starting from 260 °C is corresponding to the thermal decomposition of bbi molecule, and the tailing mass loss above ca. 330 °C may be due to the gradual elimination of accumulation carbon [74,75]. The TG curve of compound **1** shows the total mass loss of 22.86% from 400 to 600 °C, coinciding well with the calculated value of 22.78% for five bbi ligands in compound **1** with the final residue of Cu_2O and WO_3. In

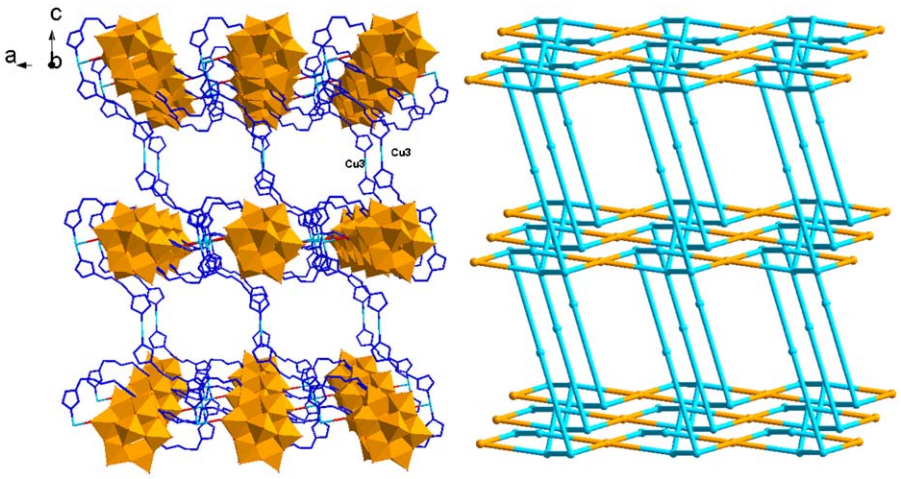

Fig. 3. Left: The combined polyhedral and ball/stick representation of the 3D framework in compound **1**. Right: The topological representation of the 3D framework. The hydrogen atoms are omitted for clarity.

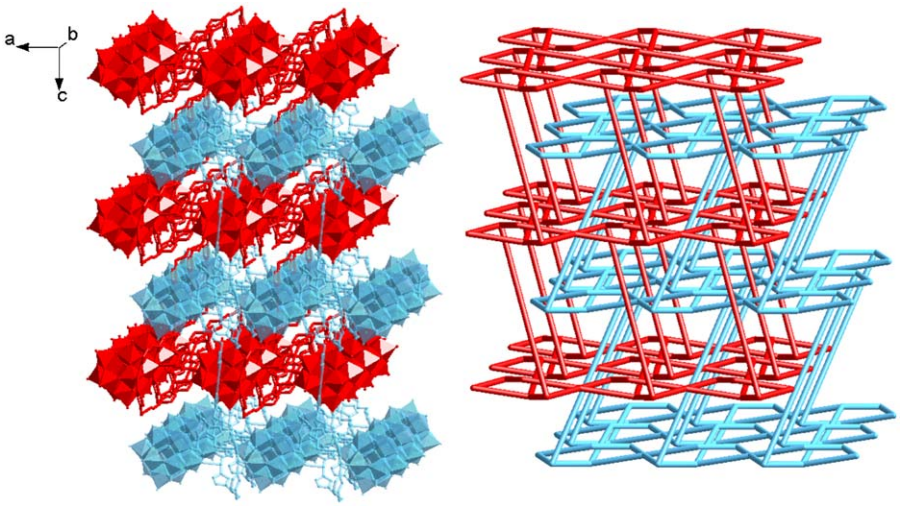

Fig. 4. Left: The combined polyhedral and ball/stick representation of the 3D+3D framework in compound **1**. Right: The topological representation of the 3D+3D framework. The hydrogen atoms are omitted for clarity.

comparison with the two TG curves, they have a similar pattern, that is, a sharp mass loss followed by a tailing. Differently, the staring temperature of thermal decomposition for bbi ligands in compound **1** is about 140 °C higher than that for free bbi molecule, and this result is expected as the coordination bonds should make the structure more stable.

Entangled structures are uncommon and much more complicated than normal structures. The study on the non-isothermal kinetics of the thermal decomposition for such compounds should be of significance for understanding their solid characters, and the TG data can provide dynamic parameters E (activation energy) and A (pre-exponential factor) for thermal decomposition of POM derivatives by using differential or integral methods developed by Friedman as well as Ozawa–Flynn–Wall [76–78].

To study the non-isothermal kinetics of the pyrolytic reaction of the bbi ligands, the TG curves of compound **1** at various heating rates were recorded (Fig. 5 left). Because the thermal events in compound **1** mainly occurred in the step of the sharp mass loss corresponding to the pyrolytic reaction of the bbi ligands, the study was based on the data of this part, and the Friedeman equation was adopted to determine the kinetic parameters:

$$\ln(dx/dt)_{x=xj} = \ln[A \cdot f(x)_j] - \mathrm{E/RT}$$

where x is the degree of conversion, dx/dt the rate of conversion, $f(x)$ the mechanism function, E the activation energy, A the pre-exponential factor, and R the gas constant. From the equation it can be seen that the graph $\ln(dx/dt)$ versus $1/T$ shows straight lines with slopes $m=-E/R$, indicating that the degree of conversion is directly proportional to E. From the slopes of these straight lines, as shown in Fig. 5 right, E could be obtained. The calculated results are shown in Table 2. Three maximums appeared in the table indicate that the pyrolytic reaction of the bbi ligands at least is a three-step process with $E_1=154.49\pm17.90\,\mathrm{kJ\,mol^{-1}}$, $\lg(A_1/\mathrm{s^{-1}})=9.11$, $E_2=126.65\pm5.15$, $\lg(A_2/\mathrm{s^{-1}})=7.33$, $E_3=138.15\pm38.64$, $\lg(A_3/\mathrm{s^{-1}})=7.55$, respectively [74,75,79–81]. We did not try to identify the intermediates in each step as the reaction is complicated and the characterization should be difficult.

3.4. Electrochemical properties

POMs possess the ability of undergoing reversible multi-electron redox processes [82], which makes them very attractive in chemically-modified electrode and the electrocatalytic study. Because the MOF-modified POM-based compounds obtained by hydrothermal conditions usually have poor solubility in water and

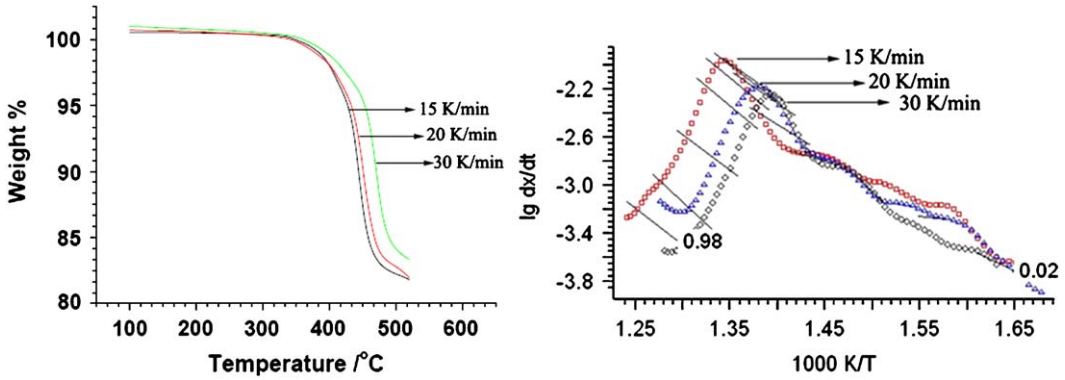

Fig. 5. Left: The TG curves of compound **1** with the heating rates of 15, 20 and 30 °C min^{-1}. Right: Friedeman analysis of the decomposition process of compound **1**.

Table 2
Kinetic parameters for the thermal decomposition of compound **1**.

Partial mass loss	E (kJ mol^{-1})	lg (A/s^{-1})
0.02	70.05 ± 1.41	2.34
0.10	154.49 ± 17.90	9.11
0.20	46.17 ± 28.23	0.79
0.30	93.20 ± 20.90	4.48
0.40	103.91 ± 13.81	5.50
0.50	108.44 ± 2.52	5.97
0.60	116.61 ± 4.17	6.62
0.70	125.49 ± 8.05	7.27
0.80	122.47 ± 2.21	7.00
0.90	112.64 ± 2.71	6.07
0.95	138.15 ± 38.64	7.55
0.98	114.82 ± 187.36	6.01

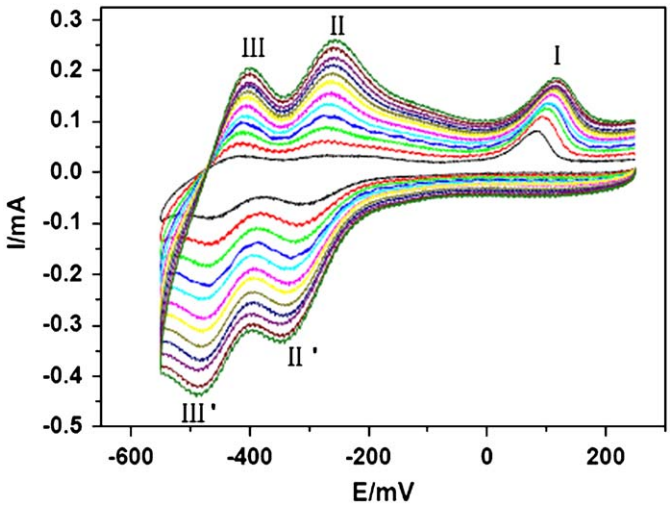

Fig. 6. The cyclic voltammograms of **1**–CPE in 1 M H_2SO_4 at the different scan rates. From inner to outer: for **1**–CPE, 40, 80, 120, 160, 200, 240, 280, 320, 360, 400, 440, 480 mV s^{-1}.

common organic solvent, so the bulk-modified carbon paste electrode method was chosen to investigate the electrochemical behavior and the electrocatalytic activity.

The **1**–CPE was prepared to study the redox property of compound **1**. The electrochemical behavior was studied in 1 M H_2SO_4 aqueous solution (Fig. 6). In the potential range of +300 to −600 mV, it can be clearly seen that, two pairs of redox peaks (II–II′, III–III′) are observed for compound **1**, with the peak potentials $E_{1/2}=(E_{pc}+E_{pa})/2-299$, −443 mV, respectively, which can be ascribed to two consecutive two electron processes of W atoms [83]. In comparison with the electrochemical behaviors of the parent W_{12} anion in acidic solution reported in the literature [84], there mainly exist one difference, namely, the reversibility is decreased in **1**–CPE. There is also an irreversible anodic peak (I) exist for **1**, which should be assigned to the oxidation of Cu(I) [50]. When the scan rate was increased, the peak potentials changed gradually: the cathodic peak potentials shift toward the negative direction and the corresponding anodic peak potentials to the positive direction. When the scan rates are lower than 120 mV s^{-1}, the peak currents were proportional to the scan rates, which indicates that the redox processes are surface-controlled, and the exchanging rate of electrons is fast; however, when the scan rates were higher than 120 mV s^{-1}, the peak currents were proportional to the square root of the scan rate, which indicates that the redox process of the CPEs are diffusion-controlled (Fig. S6) [85].

Well-known, POMs have been extensively used as the electrocatalysts in the electrocatalytic reductions, Dong, Keita, Toth and Anson have reported the examples of Keggin POMs used to catalyze the reduction progresses of nitrite and hydrogen peroxide [86–89]. Herein, **1**–CPE was used to catalyze the reduction processes of bromate and nitrite (Fig. 7). It can be seen that with the addition of bromate, both reduction peak currents increase gradually while the corresponding oxidation peak currents decrease gradually. The phenomenon suggests that the bromate is reduced by both the two-electron reduced species of W. In the reduction progress of nitrite, **1**–CPE put up the similar behavior. The facts indicate that **1**–CPE exhibits the electrocatalytic activity toward the reduction of bromate and nitrite.

4. Conclusion

In summary, a new compound based on α-metatungstate and Cu-bbi complexes has been synthesized and characterized. It represents the first example of interpenetrating based on the isopolytungstate inorganic building blocks. In compound **1**, the W_{12} clusters play the role of tetra-dentate subunits, the Cu(I) cations in the compound adopt the "T-type" and linear geometry, respectively. The structure shows a 3D (3,3,4)—connected framework with the topology of $(6^18^2)_2(6^28^210^2)$, then two such identical parts interpenetrate each other to form a twofold 3D+3D interpenetrating structure. The work enrich the α-metatungstate family and extend the area of entangle systems based on POMs. The electrochemical property of compound **1** indicates that **1**–CPE exhibits the electrocatalytic activity toward the reduction of bromate and nitrite. The non-isothermal kinetics of the thermal decomposition of compound **1** is primitively studied and for the first time reported in the POM area, providing the activation energy E and pre-exponential factor A that are

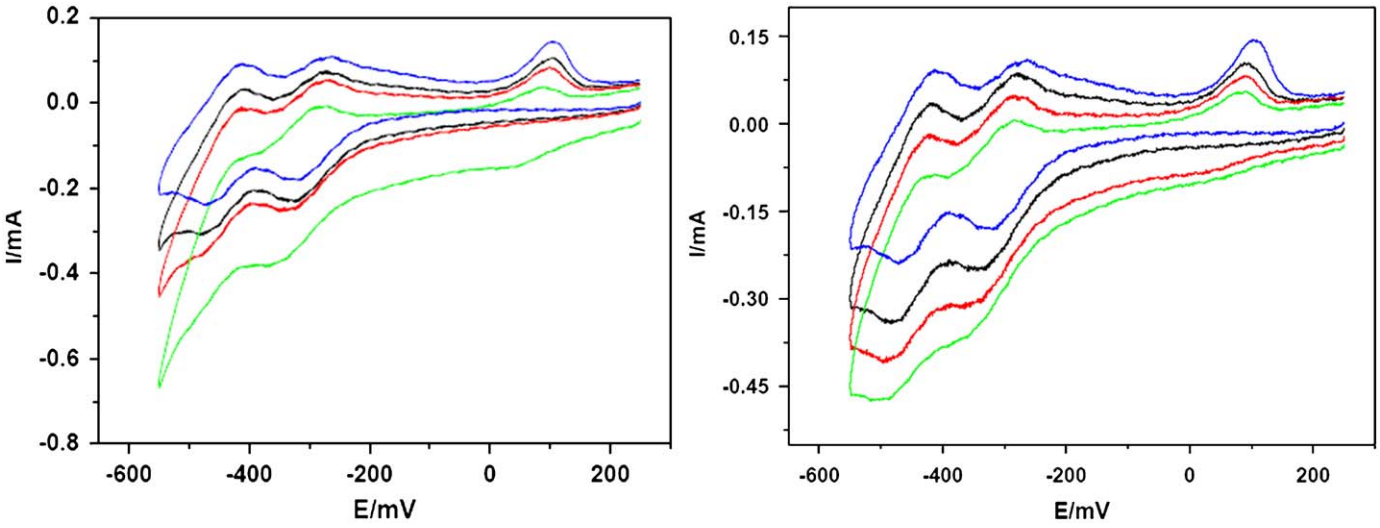

Fig. 7. Left: Cyclic voltammogram of the **1** – CPE in the 1 M H_2SO_4 aqueous solution containing 0.0, 1.0, 3.0, 5.0 mL $KBrO_3$. Right: Cyclic voltammogram of the **1** – CPE in the 1 M H_2SO_4 aqueous solution containing 0.0, 1.0, 3.0, 5.0 mL $NaNO_2$. Scan rate: 150 mV s^{-1}.

essential in estimating the thermal stabilities of compounds and furthermore for the study of thermal reaction mechanism. On the base of this thermal study, we will extend comparative investigations on non-isothermal kinetics of the thermal decomposition of other compounds with various frameworks.

Acknowledgments

This work is financially supported by the National Natural Science Foundation of China (20671016), Testing Foundation of Northeast Normal University, the Program for Changjiang Scholars and Innovative Research Team in University.

Appendix A. Supporting Information

Supplementary data associated with this article can be found in the online version at 10.1016/j.jssc.2009.09.032.

References

[1] S.J. Loeb, Chem. Commun. (2005) 1511.
[2] B.F. Abrahams, S.R. Batten, M.J. Grannas, H. Hamit, B.F. Hoskins, R. Robson, Angew. Chem. Int. Ed. 38 (1999) 1475.
[3] Y.H. Li, C.Y. Su, A.M. Goforth, K.D. Shimizu, K.D. Gray, M.D. Smith, H. Loye, Chem. Commun. (2003) 1630.
[4] M. Du, X.J. Jiang, X.J. Zhao, Chem. Commun. (2005) 5521.
[5] D.L. Long, R.J. Hill, A.J. Blake, N.R. Champness, P. Hubberstey, C. Wilson, M. Schröer, Chem. Eur. J. 11 (2005) 1384.
[6] K. Kim, Chem. Soc. Rev. 31 (2002) 96.
[7] D.F. Sun, S.Q. Ma, Y.X. Ke, D.J. Collins, H.C. Zhou, J. Am. Chem. Soc. 128 (2006) 3896.
[8] Y. Cui, S.J. Lee, W.B. Lin, J. Am. Chem. Soc. 125 (2003) 6014.
[9] L. Carlucci, G. Ciani, D.M. Proserpio, CrystEngComm 5 (2003) 269.
[10] L. Carlucci, G. Ciani, D.M. Proserpio, Chem. Commun. (2004) 380.
[11] L. Carlucci, G. Ciani, S. Maggini, D.M. Proserpio, Cryst. Growth Des. 8 (2008) 162.
[12] J.S. Miller, Adv. Mater. 13 (2001) 525.
[13] B. Kesanli, Y. Cui, M.R. Smith, E.W. Bittner, B.C. Bockrath, W. Lin, Angew. Chem. Int. Ed. 44 (2005) 72.
[14] R. Kitaura, K. Seki, G. Akiyama, S. Kitagawa, Angew. Chem. Int. Ed. 42 (2003) 428.
[15] B.L. Chen, S.Q. Ma, F. Zapata, F.R. Fronczek, E.B. Lobkovsky, H.C. Zhou, Inorg. Chem. 46 (2007) 1233.
[16] J.P. Zhang, S. Horike, S. Kitagawa, Angew. Chem. Int. Ed. 46 (2007) 889.
[17] C. Qin, X.L. Wang, L. Carlucci, M.L. Tong, E.B. Wang, C.W. Hu, L. Xu, Chem. Commun. (2004) 1876.
[18] X.H. Bu, M.L. Tong, H.C. Chang, S. Kitagawa, S.R. Batten, Angew. Chem. Int. Ed. 43 (2004) 192.
[19] B.L. Chen, C.D. Liang, J. Yang, D.S. Contreras, Y.L. Clancy, E.B. Lobkovsky, O.M. Yaghi, S. Dai, Angew. Chem. Int. Ed. 45 (2006) 1390.
[20] J.P. Zhang, Y.Y. Lin, W.X. Zhang, X.M. Chen, Angew. Chem. Int. Ed. 127 (2005) 14162.
[21] L. Carlucci, G. Ciani, D.M. Proserpio, Coord. Chem. Rev. 246 (2003) 247.
[22] S.R. Batten, R. Robson, Angew. Chem. Int. Ed. 37 (1998) 1460.
[23] S.R. Batten, CrystEngComm 18 (2001) 1.
[24] X.L. Wang, C. Qin, E.B. Wang, Y.G. Li, Z.M. Su, Chem. Commun. (2005) 5450.
[25] X.L. Wang, C. Qin, E.B. Wang, Y.G. Li, Z.M. Su, L. Xu, L. Carlucci, Angew. Chem. Int. Ed. 44 (2005) 5824.
[26] X.L. Wang, C. Qin, E.B. Wang, Z.M. Su, Chem. Eur. J. 12 (2006) 2680.
[27] X.L. Wang, C. Qin, E.B. Wang, L. Xu, Z.M. Su, C.W. Hu, Angew. Chem. Int. Ed. 43 (2004) 5036.
[28] Y.Q. Lan, S.L. Li, J.S. Qin, D.Y. Du, X.L. Wang, Z.M. Su, Q. Fu, Inorg. Chem. 47 (2008) 10600.
[29] Y.F. Hsu, C.H. Lin, J.D. Chen, J.C. Wang, Cryst. Growth Des. 8 (2008) 1094.
[30] M. Du, X.J. Jiang, X.J. Zhao, Inorg. Chem. 46 (2007) 3984.
[31] G.H. Wang, Z.G. Li, H.Q. Jia, N.H. Hu, J.W. Xu, Cryst. Growth Des. 8 (2008) 1932.
[32] Y. Qi, Y.X. Che, J.M. Zheng, Cryst. Growth Des. 8 (2008) 3602.
[33] M.H. Mir, S. Kitagawa, J.J. Vittal, Inorg. Chem. 47 (2008) 7728.
[34] A. Müller, F. Peters, M.T. Pope, D. Gatteschi, Chem. Rev. 98 (1998) 239.
[35] C.Y. Sun, S.X. Liu, D.D. Liang, K.Z. Shao, Y.H. Ren, Z.M. Su, J. Am. Chem. Soc. 131 (2009) 1883.
[36] E. Coronado, C. Giménez-Saiz, C.J. Gómez-García, Coord. Chem. Rev. 249 (2005) 1776.
[37] S. Uchida, R. Kawamoto, H. Tagami, Y. Nakagawa, N. Mizuno, J. Am. Chem. Soc. 130 (2008) 12370.
[38] T. Yamase, J. Chem. Soc. Dalton Trans. (1985) 2585.
[39] X.H. Wang, J.F. Liu, M.T. Pope, Dalton Trans. (2003) 957.
[40] E. Coronado, J.R. Galán-Mascarós, C. Giménez-Saiz, C.J. Gómez-García, E. Martínez-Ferrero, M. Almeida, E.B. Lopes, Adv. Mater. 16 (2004) 324.
[41] Z.M. Zhang, Y.G. Li, S. Yao, E.B. Wang, Y.H. Wang, R. Clérac, Angew. Chem. Int. Ed. 48 (2009) 1581.
[42] D.L. Long, E. Burkholder, L. Cronin, Chem. Soc. Rev. 36 (2007) 105.
[43] B.X. Dong, J. Peng, C.J. Gómez-García, S. Benmansour, H.Q. Jia, N.H. Hu, Inorg. Chem. 46 (2007) 5933.
[44] J.Q. Sha, J. Peng, Y.Q. Lan, Z.M. Su, H.J. Pang, A.X. Tian, P.P. Zhang, M. Zhu, Inorg. Chem. 47 (2008) 5145.
[45] A.X. Tian, J. Ying, J. Peng, J.Q. Sha, H.J. Pang, P.P. Zhang, Y. Chen, M. Zhu, Z.M. Su, Inorg. Chem. 48 (2009) 100.
[46] C. Ritchie, E.M. Burkholder, D.L. Long, D. Adam, P. Kögerlerb, L. Cronin, Chem. Commun. (2007) 468.
[47] C. Ritchie, E. Burkholder, P. Kögerlerb, L. Cronin, Dalton Trans. (2006) 1712.
[48] H.Y. An, E.B. Wang, D.R. Xiao, Y.G. Li, Z.M. Su, L. Xu, Angew. Chem. Int. Ed. 45 (2006) 904.
[49] V. Shivaiah, M. Nagaraju, S.K. Das, Inorg. Chem. 42 (2003) 6604.
[50] A.X. Tian, J. Ying, J. Peng, J.Q. Sha, Z.G. Han, J.F. Ma, Z.M. Su, N.H. Hu, H.Q. Jia, Inorg. Chem. 47 (2008) 3274.
[51] J.Q. Sha, J. Peng, A.X. Tian, H.S. Liu, J. Chen, P.P. Zhang, Z.M. Su, Cryst. Growth Des. 7 (2007) 2535.
[52] C.J. Zhang, Y.G. Chen, H.J. Pang, D.M. Shi, M.X. Hu, J. Li, Inorg. Chem. Commun. 11 (2008) 765.
[53] C. Streb, C. Ritchie, D.L. Long, P. Kögerler, L. Cronin, Angew. Chem. Int. Ed. 46 (2007) 7579.

[54] B.Z. Lin, Z. Li, L.W. He, L. Bai, X.F. Huang, Y.L. Chen, Inorg. Chem. Commun. 10 (2007) 600.
[55] C. Qin, X.L. Wang, E.B. Wang, Z.M. Su, Inorg. Chem. 47 (2008) 5555.
[56] C. Qin, X.L. Wang, L. Yuan, E.B. Wang, Cryst. Growth Des. 8 (2008) 2093.
[57] Y.Q. Lan, S.L. Li, X.L. Wang, K.Z. Shao, Z.M. Su, E.B. Wang, Inorg. Chem. 47 (2008) 529.
[58] Y.Q. Lan, S.L. Li, X.L. Wang, K.Z. Shao, D.Y. Du, H.Y. Zang, Z.M. Su, Inorg. Chem. 47 (2008) 8179.
[59] X.L. Wang, C. Qin, E.B. Wang, Z.M. Su, Chem. Commun. (2007) 4245.
[60] S.L. Li, Y.Q. Lan, J.F. Ma, J. Yang, X.H. Wang, Z.M. Su, Inorg. Chem. 46 (2007) 8283.
[61] J.F. Ma, J. Yang, G.L. Zheng, L. Li, J.F. Liu, Inorg. Chem. 42 (2003) 7531.
[62] G.M. Sheldrick, SHELXL-97, Program for Crystal Structure Refinement, University of Göttingen, Germany, 1997.
[63] G.M. Sheldrick, SHELXL-97, Program for Crystal Structure Solution, University of Göttingen, Germany, 1997.
[64] I.D. Brown, D. Altermatt, Acta Crystallogr. Sect. B (1985) 4124.
[65] C.D. Wu, C.Z. Lu, H.H. Zhuang, J.S. Huang, Inorg. Chem. 41 (2002) 5636.
[66] Z.Y. Shi, X.J. Gu, J. Peng, X. Yu, E.B. Wang, Eur. J. Inorg. Chem. (2006) 385.
[67] C.R. Sprangers, J.K. Marmon, D.C. Duncan, Inorg. Chem. 45 (2006) 9628.
[68] S.T. Zheng, J. Zhang, G.Y. Yang, Inorg. Chem. 44 (2005) 2426.
[69] S.T. Zheng, M.H. Wang, G.Y. Yang, Inorg. Chem. 46 (2007) 9503.
[70] C.L. Wang, S.X. Liu, L.H. Xie, Y.H. Ren, D.D. Liang, C.Y. Sun, H.Y. Cheng, Polyhedron 26 (2007) 3017.
[71] L.L. Fan, D.R. Xiao, E.B. Wang, Y.G. Li, Z.M. Su, X.L. Wang, J. Liu, Cryst. Growth Des. 7 (2007) 592.
[72] H.Q. Tan, Y.G. Li, Z.M. Zhang, C. Qin, X.L. Wang, E.B. Wang, Z.M. Su, J. Am. Chem. Soc. 129 (2007) 10066.
[73] R. Thouvenot, M. Fournier, R. Franck, C. Rocchiccioli-Deltcheff, Inorg. Chem. 23 (1984) 598.
[74] X.Q. Shen, H.J. Zhong, H. Zheng, H.Y. Zhang, G.H. Zhao, Q.A. Wu, H.Y. Mao, E.B. Wang, Y. Zhu, Polyhedron 23 (2004) 1851.
[75] H.X. Yang, X.R. Meng, Y. Liu, H.W.i. Hou, Y.T. Fan, X.Q. Shen, J. Solid State Chem. 181 (2008) 2178.
[76] T. Ozawa, Bull. Chem. Soc. Jpn. 38 (1965) 1881.
[77] J.H. Flynn, J. Polym. Sci. Part B 4 (1966) 323.
[78] H.L. Friedman, J. Polym. Sci. Part C 6 (1963) 183.
[79] S. Vyazovkin, Int. Rev. Phys. Chem. 19 (2000) 45.
[80] S. Vyazovkin, W. Linert, Int. J. Chem. Kinet. 27 (1995) 73.
[81] S. Vyazovkin, C.A. Wight, Thermochim. Acta 340 (1999) 53.
[82] X.D. Xi, G. Wang, B.F. Liu, S.J. Dong, Electrochim. Acta 40 (1995) 1025.
[83] M. Sadakane, E. Steckhan, Chem. Rev. 98 (1998) 219.
[84] B. Ketta, L. Nadjo, J. Electroonoi. Chem. 223 (1987) 287.
[85] Z.G. Han, Y.L. Zhao, J. Peng, Q. Liu, E.B. Wang, Electrochim. Acta 51 (2005) 218.
[86] J.E. Toth, F.C. Anson, J. Am. Chem. Soc. 111 (1989) 2444.
[87] S.J. Dong, X.D. Xi, M. Tian, J. Electroanal. Chem. 385 (1995) 227.
[88] B. Keita, A. Belhouari, L. Nadjo, R. Contant, J. Electroanal. Chem. 381 (1995) 243.
[89] J.E. Toth, F.C. Anson, J. Electroanal. Chem. 256 (1988) 361.